International Journal of
Plasma Environmental Science and Technology

Regular Paper DOI: 10.34343/ijpest.2024.18.e02004

Control of bubble motion in dielectric liquid by traveling-wave nonuniform electric fields

Toru Oda[1,*], Toshiyuki Kawasaki[1], Seiji Kanazawa[2]

[1] Department of Electrical and Electronic Engineering, Nishinippon Institute of Technology, Japan
[2] Department of Science and Technology, Oita University, Japan

* Corresponding author: oda@nishitech.ac.jp (Toru Oda)

Received: 31 May 2024
Revised: 23 July 2024
Accepted: 28 July 2024
Published online: 2 August 2024

Abstract
The dynamic behavior of air bubbles in liquid has recently attracted interest in space utilization. Although the motion of bubbles is not easy to control in a terrestrial environment due to strong buoyant force, we have succeeded in regulating their movement in kerosene by applying a low-frequency traveling-wave electric field through an electric curtain that is installed horizontally in the kerosene. The bubbles ascending due to buoyant force are obstructed by the electrodynamical gradient force from the electric curtain and transported by Coulomb's force in the direction parallel to the traveling-wave at a velocity about five times higher than the ascending velocity. Air bubbles accumulate near the electrode train at approximately three times the electrode pitch and move together as a group. The results of electrodynamical computer simulations of bubbles under buoyancy exhibit favorable agreement with the experimental results.

Keywords: Electrohydrodynamics, traveling-wave electric field, bubble motion, electric field curtain, kerosene.
.

1. Introduction

Recent scientific and technological advances have increased the importance of space exploration. Materials behave differently in a microgravity environment compared with on Earth, affecting the operation of spacecraft and space stations. Materials such as fine particles, debris, or droplets float in space. Dust and sand, which are fine particles, may adhere to solar panels and reduce the efficiency of power generation; thus, such deposited particles must be removed [1]. Debris can damage spacecrafts and space stations upon collision; hence, methods to avoid such situations are being studied [2]. Bubbles, which are the focus of this research, are formed in the presence of a liquid and affect the behavior of the fluid. The control of bubbles in microliquids is important in space application technology for microgravity environments, and the behavior of bubbles generated in droplets has been previously observed [3]. In ground-based experiments, buoyancy is the primary mechanical effect of bubbles under 1G (gravitational acceleration G = 9.81 m s^{-2}). Controlling bubble motion or reducing buoyancy is generally difficult. In a microgravity environment, moreover, the liquid can move freely and further affect the behavior of bubbles. In particular, bubbles in fuel liquids can adversely affect engine performance and safety. As a solution to such problems, the electrohydrodynamic effect can be utilized to control the dynamics and separation of liquids.

Detailed experiments on the electrohydrodynamic effects of bubbles formed in a dielectric liquid in an AC nonuniform traveling-wave electric field qualitatively revealed that a traveling-wave electric field curtain placed in kerosene can prevent the upward motion of a fine bubble group (0.2 mm in diameter) due to buoyancy and transport the bubble group in the traveling-wave direction [4]. In particular, in the theoretical analysis, the stagnant and traveling modes of bubbles could be explained by controlling the frequency and applied phase voltage of the three-phase AC high-voltage power supply, but the phenomenon of discontinuous movement at three times the electrode pitch could not be explained. This observation can be attributed to the bubbles in kerosene being charged by the surrounding electric double layer formed at the gas–liquid interface. In addition, the discontinuous movement is thought to be caused by the interaction between the electrodynamic confining and driving forces of the traveling-wave electric field formed in the kerosene by the electric field curtain in the vicinity of the electrode row.

In this paper, we report a detailed visualization of bubble motion in a traveling-wave electric field and a computer simulation with a high approximation degree of the electric field to explain the observed results, allowing for the quantitative analysis of each mode.

2. Experimental setup and method

Figs. 1 and 2 show the basic experimental setup comprising a single planar electric field curtain [5] placed horizontally in kerosene. The electric field curtain was formed by placing a row of 111 Teflon-coated cylindrical electrodes (2 mm in diameter and 185 mm in length) parallel to an insulating plastic frame (360 mm long and 220 mm wide) with an electrode spacing (pitch) of 2.5 mm. The parallel cylindrical electrode rows were connected to a frequency-variable three-phase AC high-voltage power supply (Pulse Electronics Co., Ltd.) to form a traveling-wave electric field. High-voltage sinusoidal waves with a 120° phase difference were generated by boosting the voltage from three high-voltage vacuum tube amplifiers (Eimac 4-400A, made in USA) with three transformers. The frequency of the high voltage varied in the range of 5–50 Hz, and its amplitude was adjusted in the range of 0–15 kV and applied to the electrode train. The applied voltage and frequency were measured with an oscilloscope (Tektronix TDS 540D) using a 2000:1 voltage divider connected to the high-voltage electrodes (only one phase is shown in Fig. 2).

For the observation of bubble motion, a row of parallel cylindrical electrodes was placed 200 mm above a transparent acrylic container (450 mm × 300 mm × 300 mm). Small bubbles (0.2 mm in diameter) were supplied by an air stone placed at the bottom of the acrylic container. Bubble motion was observed using a video camera (SONY, CCD-TR75), and the captured images were quantitatively analyzed using a playback system attached to the video camera. The method for measuring the terminal velocity of bubbles was to use a stopwatch to measure the traveling time from the moment a group of bubbles generated from the lower air stone reaches the upper electrode to the terminal electrode row (15 cm from the center) and calculated the velocity.

Commercial kerosene (approximately 34 L in volume) was used as the insulating liquid. Its physical properties were a relative permittivity ε_m between 2.5 and 3, an electrical conductivity σ_m of 10^{-13} S m^{-1}, and a liquid kinematic viscosity ν_m of 2×10^{-6} m^2 s^{-1} at room temperature. Although liquid viscosity varies with temperature, the experiments were conducted in nearly constant room temperature (20 °C–25 °C); thus, the change in liquid viscosity is negligible.

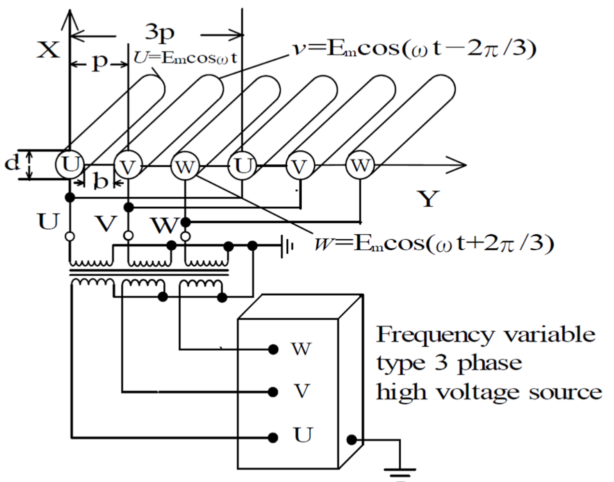

Fig. 1. Series of parallel cylindrical electrodes applied with three-phase voltage.

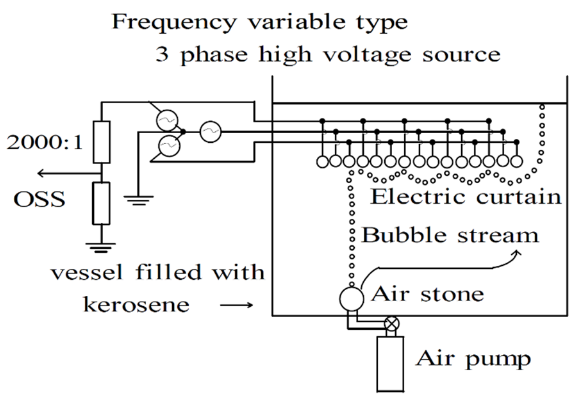

Fig. 2. Experimental configuration

3. Experimental results and discussion

3.1 Observation of bubble motion in liquid

Fig. 3 shows the bubbles rising in kerosene due to buoyancy and slipping through the gap between the cylindrical wire electrodes when no voltage is applied (i.e., slip-through mode). However, Fig. 4(a) illustrates that the bubbles from the air-stone are blocked right in front of the row of parallel cylindrical electrodes upon the application of low-frequency three-phase AC high voltage and are transported in the same direction as the traveling wave (i.e., transport mode). In this case, the applied voltage is 8 kV and the frequency is 8 Hz. The formed bubbles have a diameter of approximately 0.2 mm. Notably, they do not move continuously and smoothly but rather form groups based on a spatial period that is three times the electrode pitch and maintain their discontinuous movement. Fig. 4(b) shows the moment when the voltage is abruptly turned off from the transport mode. A few seconds later, it enters the slip-through mode, as shown in Fig. 3.

Applying Stokes' law acting on a spherical object of very small Reynolds number in a viscous fluid, the ascent velocity of a bubble due to buoyancy in kerosene, V_b, is obtained by

$$V_\mathrm{b} = \frac{\rho_\mathrm{m} V \mathrm{g}}{6\pi\, \eta_\mathrm{m}\, a} \tag{1}$$

where $\rho_m = 800$ kg m^{-3} is the density of the liquid, g is the acceleration of gravity [m s^{-2}], V is the volume of the bubble [m^3], $\eta_m = 1.63 \times 10^{-3}$ N s m^{-2} is the viscosity of the liquid, and a is the radius of the bubble [m].

From Eq. (1), the ascent velocity V_b of a bubble of 0.2 mm in diameter in kerosene is 0.018 m s^{-1} (1.8 cm s^{-1}), which agrees well with the observation. The corresponding Reynolds number is 1.8. From the video observations, the horizontal movement velocity of the bubbles is approximately four to five times the ascent velocity V_b. In addition, a stagnant mode appears in which the bubbles stop moving when the applied voltage and frequency reach a certain range. The bubbles that are blocked in front of the electrodes behave as if they are a standing wave electric field and are retained despite the presence of a traveling-wave electric field. Fig. 5 (a) shows that no bubbles have slipped through the gap between the electrodes. In this case, the applied voltage and frequency are 8 kV and 20 Hz, respectively. Fig. 5 (b) shows that when the applied voltage is turned off abruptly from this state, the previously stagnant air bubbles slip through the gaps between the electrodes, thus forming an electric field curtain. A few seconds later, the slip-through mode shown in Fig. 3 is achieved.

The phenomenon of liquid pumping by a traveling-wave electric field in a semi-insulating liquid has been observed by Melcher [6]. In this case, a 60 Hz 6-phase power source was used, However, the bubble motion, as in this study, is not taken into account

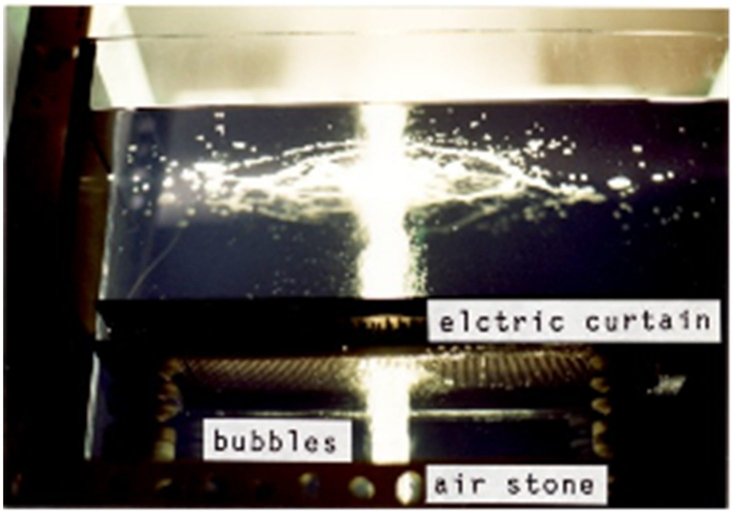

Fig. 3. Slip-through mode (No voltage is applied).

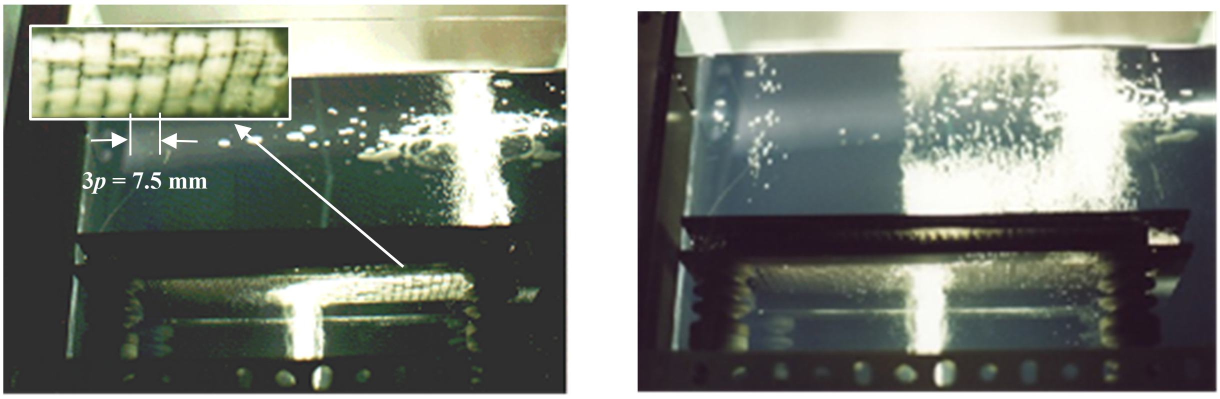

(a) (b)

Fig. 4. (a) Traveling mode at 8 kV and 8 Hz and (b) moment when the voltage was turned off from the transport.

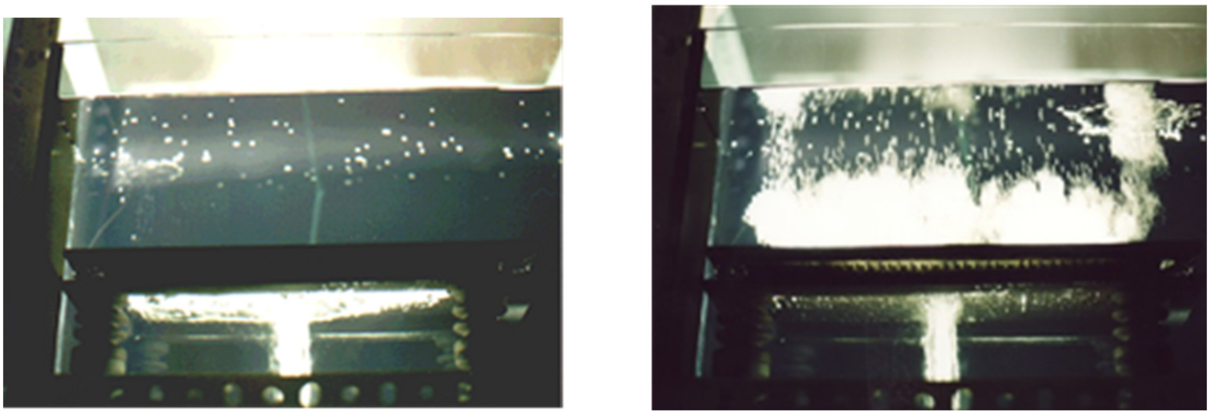

(a) (b)

Fig. 5. (a) Stagnation mode at 8 kV and 20 Hz and (b) moment when the voltage was turned off from the stagnation mode.

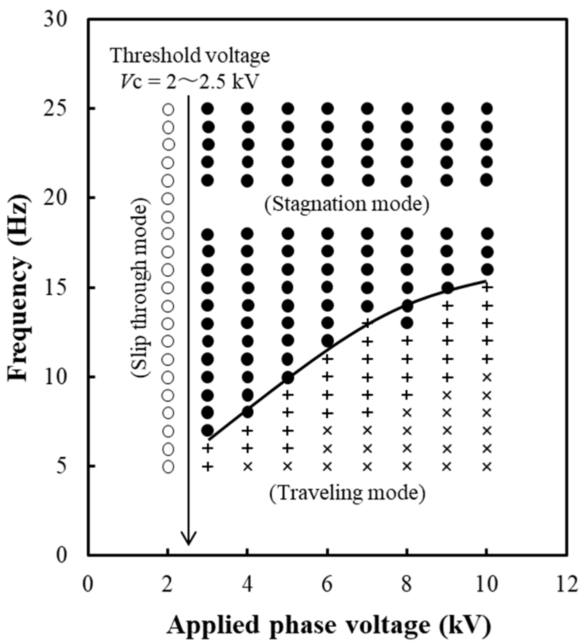

Fig. 6. Characteristics of bubble motion.

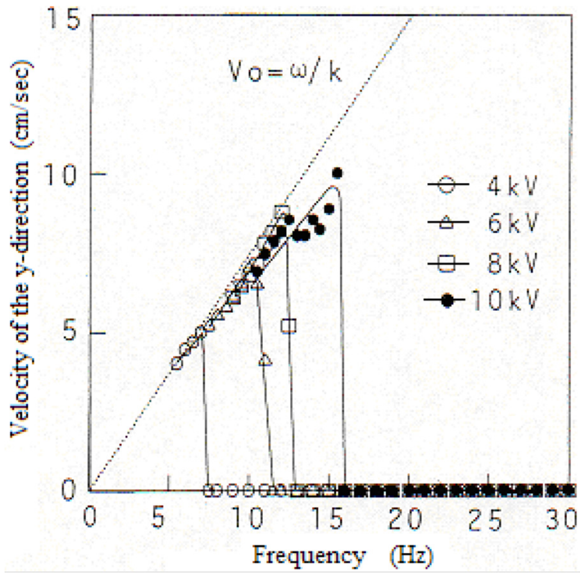

Fig. 7. Bubble drift velocity.

3.2 Frequency dependence of bubble motion and transport velocity

Fig. 6 shows the relationship between frequency and voltage for the bubble motion mode in kerosene. In this experiment, the voltage varies from 0 to 8 kV and the frequency varies from 5 Hz to 50 Hz. The stagnant mode is in the region marked with a closed circle (●). In this region, the bubbles only oscillate slightly in front of the electrode and do not move. Bubbles in the stagnant mode do not slip through the gap between the cylindrical electrodes, as shown in Fig. 5 (a). The area on the left marked with an open circle (○) is the area where all the ascending bubbles slip through the gap between the electrodes. Solid lines are drawn at the boundary between the transport mode and the stagnation mode. Preliminary experiments show that ~2.5 kV is the threshold voltage at which bubbles are prevented from slipping, and this value is independent of frequency. The area marked with a plus symbol (+) indicates the transport mode in which bubbles are transported in the same direction as the phase order of the applied voltage. The area marked with (×) is the area where experiments cannot be performed due to the performance of the power supply device.

Fig. 7 plots the measured velocity of the moving bubbles versus power supply frequency. The parameter is the amplitude of the applied voltage. The movement speed of the bubbles is independent of the applied voltage and coincides with the characteristic $V_0 = \omega/k$ (propagation velocity of the electric field, ω is angular frequency [rad s^{-1}], k is wavenumber [m^{-1}]) as the frequency increases. The terminal velocity of the bubbles increased with increasing the frequency, with values ranging from about 4 to 10 cm s^{-1}. Similar phenomena have been observed in the transport of charged particles by a traveling-wave electric field curtain in air, such as the particle transport when the average velocity is equal to the wave speed [7]. These characteristics of bubble motion could be pertinent in microgravity environments for space applications, such as eliminating incomplete combustion by removing a group of bubbles generated in liquid fuel, or applications in chemistry, such as controlling the bubble dwell time in a liquid.

4. Theoretical considerations

4.1 Equation of motion for bubbles

The electric force F acting on a gas–liquid mixed phase due to a nonuniform electric field is generally expressed by [8]

$$
\begin{aligned}
F = {} & QE - \frac{1}{2}\varepsilon_0 E^2 \cdot \mathrm{grad}(\varepsilon_\mathrm{m}) \cdot \frac{4}{3}\pi a^3 \\
& + \frac{1}{2}\mathrm{grad}\left(E^2\, \varepsilon_0\, \rho_\mathrm{m} \frac{d\varepsilon_\mathrm{m}}{d\rho_\mathrm{m}}\right) \cdot \frac{4}{3}\pi a^3 \\
& + 2\pi a^3 \frac{\varepsilon_\mathrm{s} - \varepsilon_\mathrm{m}}{\varepsilon_\mathrm{s} + 2\varepsilon_\mathrm{m}} \varepsilon_0 \varepsilon_\mathrm{m} \cdot \mathrm{grad}(E^2) \quad ,
\end{aligned}
\tag{2}
$$

where a is the radius of the bubble [m], ε_s is the relative permittivity of the bubble [−], ε_m is the relative permittivity of the liquid [−], ε_0 is the permittivity of the vacuum [F m^{-1}], Q is the charge of the bubble [C], and ρ_m is the density of the liquid [kg m^{-3}]. On the right hand side of Eq. (2), the first term is either the Coulomb force due to the net space charge density or the electrophoretic force due to the true charge density of the bubble. The second term is the force produced when the dielectric constant of the liquid changes with a change in space, and the third term is the force generated when the dielectric constant of the liquid changes with the liquid density ρ_m. The fourth term represents the gradient force (tilt force) due to the differences in the dielectric constants ε_s and ε_m of bubbles and liquids.

The equations of bubble motion are analyzed by considering only the Coulomb and gradient forces in the first and fourth terms. The second and third terms can be neglected because the bubble radius is small. The following three-phase traveling-wave potential function is used to calculate the electric field [5]:

$$
\begin{aligned}
V(x, y, t) = {} & E_{03}\ \left\{ \sum_{\mathrm{m}=1,4,7,\cdots}^{\infty} \frac{1}{\mathrm{m}\,k} \exp[-\mathrm{m}\,k\,|x|\,] \cos[\theta + \mathrm{m}\,k\,R_0] \right. \\
& \left. \cos[\omega t - \mathrm{m}\,k\,y] \right\} + E_{03}\ \left\{ \sum_{\mathrm{m}=2,5,8,\cdots}^{\infty} \frac{1}{\mathrm{m}\,k} \exp[-\mathrm{m}\,k\,|x|] \right. \\
& \left. \cos[\theta - \mathrm{m}\,k\,R_0]\ \cos[\omega t - \mathrm{m}\,k\,y] \right\} ,
\end{aligned}
\tag{3}
$$

This equation is a potential function that uses the principal three-phase conjugate fundamental charge sequence via the substituted charge method. The strength of the electric field in x and y directions is given by

$$\begin{aligned} E_x(x,y,t) &= -\frac{\partial V(x,y,t)}{\partial x} \\ &= E_{03}\ \Big\{ \sum_{\mathrm{m}=1,4,7,\cdots}^{\infty} \exp[-\mathrm{m}\,k\,|x|\,]\cos[\theta + \mathrm{m}\,k\,R_0] \\ &\cos[\omega t - \mathrm{m}\,k\,y] \Big\} + E_{03}\ \Big\{ \sum_{\mathrm{m}=2,5,8,\cdots}^{\infty} \exp[-\mathrm{m}\,k\,|x|] \\ &\cos[\theta - \mathrm{m}\,k\,R_0]\ \cos[\omega t - \mathrm{m}\,k\,y] \Big\} \end{aligned} , \tag{4}$$

$$\begin{aligned} E_y(x,y,t) &= -\frac{\partial V(x,y,t)}{\partial y} \\ &= -E_{03}\ \Big\{ \sum_{\mathrm{m}=1,4,7,\cdots}^{\infty} \exp[-\mathrm{m}\,k\,|x|\,]\cos[\theta + \mathrm{m}\,k\,R_0] \\ &\sin[\omega t - \mathrm{m}\,k\,y] \Big\} + E_{03}\ \Big\{ \sum_{\mathrm{m}=2,5,8,\cdots}^{\infty} \exp[-\mathrm{m}\,k\,|x|] \\ &\cos[\theta - \mathrm{m}\,k\,R_0]\ \sin[\omega t - \mathrm{m}\,k\,y] \Big\} \end{aligned} , \tag{5}$$

where the pitch between the electrodes is p = 2.5 mm, the wavenumber is $k = 2\pi/3p$ [m^{-1}], the coefficient that summarizes each constant by the applied voltage and substitute charge method is $E_{03} = 2\sqrt{6}kUA_{\mathrm{m}}$, and the effective value of the line voltage is $U = \sqrt{3}E_{\mathrm{m}}/\sqrt{2}$ [V].

Each parameter in Eqs. (4) and (5) is determined from the following electrode parameters selected from the dimensions of previous field curtains [9].

Optimal distance from electrode center to substitute charge: R_0 = 0.075 mm,

Phase difference: $\theta = 14.06 \times \pi/60$ rad,

Constant: A_{m} = 0.075,

where for m =1, 4, 7, ⋯, it proceeds in a counterclockwise rotation in the positive direction of y, and for m = 2, 5, 8, ⋯, it proceeds in a clockwise rotation in the negative direction of y.

The gradient force in the fourth term is important for gas–liquid mixed phases. When $\varepsilon_{\mathrm{s}} < \varepsilon_{\mathrm{m}}$, the bubble moves toward the weaker electric field. The x and y components of the gradient force are as follows:

$$F_{gx} = 2\pi a^3 \frac{\varepsilon_{\mathrm{s}} - \varepsilon_{\mathrm{m}}}{\varepsilon_{\mathrm{s}} + 2\varepsilon_{\mathrm{m}}}\,\varepsilon_0\,\varepsilon_{\mathrm{m}} \frac{\partial(E_x^2 + E_y^2)}{\partial x} , \tag{6}$$

$$F_{gy} = 2\pi a^3 \frac{\varepsilon_{\mathrm{s}} - \varepsilon_{\mathrm{m}}}{\varepsilon_{\mathrm{s}} + 2\varepsilon_{\mathrm{m}}}\,\varepsilon_0\,\varepsilon_{\mathrm{m}} \frac{\partial(E_x^2 + E_y^2)}{\partial y} . \tag{7}$$

One of the objectives of this study is to accurately describe the electrodynamic behavior of bubbles in kerosene under the action of a traveling-wave electric field. For this purpose, the following equations of motion (Eqs. (8) and (9)) must be solved by considering all the abovementioned forces acting on bubbles.

$$M_{\mathrm{e}}\frac{d^2x}{dt^2} + 6\pi\eta_{\mathrm{e}} a\frac{dx}{dt} = F_{\mathrm{e}x} + F_{gx} + M_{\mathrm{s}}\,\mathrm{g} , \tag{8}$$

$$M_{\mathrm{e}}\frac{d^2y}{dt^2} + 6\pi\eta_{\mathrm{e}} a\frac{dy}{dt} = F_{\mathrm{e}y} + F_{gy} , \tag{9}$$

where M_{e} is the equivalent mass of the bubble, η_{e} is the equivalent viscosity coefficient of bubble, $F_{\mathrm{e}x}$ is the Coulomb force in the x-direction, F_{ey} is the Coulomb force in the y-direction, $F_{\mathrm{g}x}$ is the gradient force in the x-

direction, F_{gy} is the gradient in the y-direction, and M_s is the apparent mass of the bubble. The equivalent mass M_e of a bubble is given by Eq. (10), which adds 1/2 of the mass of the liquid (kerosene), M_m, excluded from its volume, to the mass of the bubble itself, M_a, which is related to buoyancy [10], and also includes the effect caused by a bubble in sinusoidal oscillatory motion in a viscous liquid that also accelerates the surrounding medium (liquid) [11]. On the other hand, η_e is expressed by Eq. (11). The apparent mass M_s of the bubble is not the equivalent mass itself in Eq. (10) because the buoyancy force acting on the bubble is not an oscillatory force, but rather Eq. (12), which omits the terms related to angular frequency.

$$M_e = M_a + M_m\left(\frac{1}{2} + \frac{9}{4aS}\right) \quad , \quad S = \sqrt{\frac{\omega \rho_m}{2\eta_m}} \quad , \tag{10}$$

$$\eta_e = \eta_m + \frac{1}{6\pi a}\frac{9 M_m \omega}{4aS} \quad , \tag{11}$$

$$M_s = M_a + \frac{M_m}{2} \quad . \tag{12}$$

Owing to the nonuniform electric field, the equations of motion are nonlinear differential equations; thus, the electric field functions in Eqs. (4) and (5) vary in magnitude and direction depending on the location. The solutions to this equation are complex and cannot be obtained analytically. Therefore, numerical computer simulations are required to obtain approximate solutions. "*Mathematica* Ver. 5.0" is used for the computer simulations.

4.2 Comparison of computer simulations with experimental results

Prior to a computer simulation of bubble motion, the true charge of the bubble must be determined. According to Jones [12] and Wu [13], bubbles have a negative excess polarized charge due to the electric double layer at the gas–liquid phase interface.

Experiments using the Millikan method [14] to measure the charge of bubbles revealed a high degree of variation, with $Q \approx 10^{-11}$ to 10^{-13} C. Therefore, we use Rayleigh's theory (Eq. (13)) to determine the amount of charge Q from the equilibrium condition between the surface tension and the electrostatic repulsive force acting on the surface of a solitary charged liquid in the gas phase [15]:

$$Q = \sqrt{64\pi^2 \varepsilon_0 \gamma a^3} \quad , \tag{13}$$

where γ is the surface tension of kerosene, which is 26×10^{-3} N m^{-1}. From Eq. (13), the amount of charge on a bubble of 0.2 mm diameter is $Q \approx 10^{-11}$ C. Other parameters used in the computer simulation are as follows:

$\rho_a = 1.3$ kg m^{-3} is the air density, $\rho_m = 800$ kg m^{-3} is kerosene density, $\varepsilon_0 = 8.85 \times 10^{-12}$ F m^{-1}, $\varepsilon_s = 1.0$ is the relative dielectric constant of air, $\varepsilon_m = 2.5$ is the relative dielectric constant of kerosene, $M_a = 4/3\pi a^3 \rho_a$ [kg] is the mass of bubble, $\eta_m = 1.63 \times 10^{-3}$ N s m^{-2} is kerosene viscosity coefficient.

Fig. 8 shows one example of bubble motion trajectory from a computer simulation based on Eqs. (8) and (9). Fig. 8 (a) displays the simple upward motion due to buoyancy when no voltage is applied, and Fig. 8 (b) indicates the transport mode. The jumps of the bubble trajectory are quantitative and accurate with a spatial period of $3p = 7.5$ mm, which is consistent with the experimentally observed transport mode (Fig. 4 (a)). Fig. 8(c) shows the stagnation mode, which is observed mainly in the high frequency region and can be considered the electrohydrodynamic levitation of bubbles.

Earnshaw's theorem [16, 17] states that charged particles and bubbles cannot remain stable at electrostatic potentials. However, current computer simulations and experimental results indicate that bubbles with a true electric charge formed by the electric double layer can be stabilized by a traveling-wave electric field while maintaining a small circular motion. Fig. 9 shows the boundaries between the stagnant and transport modes

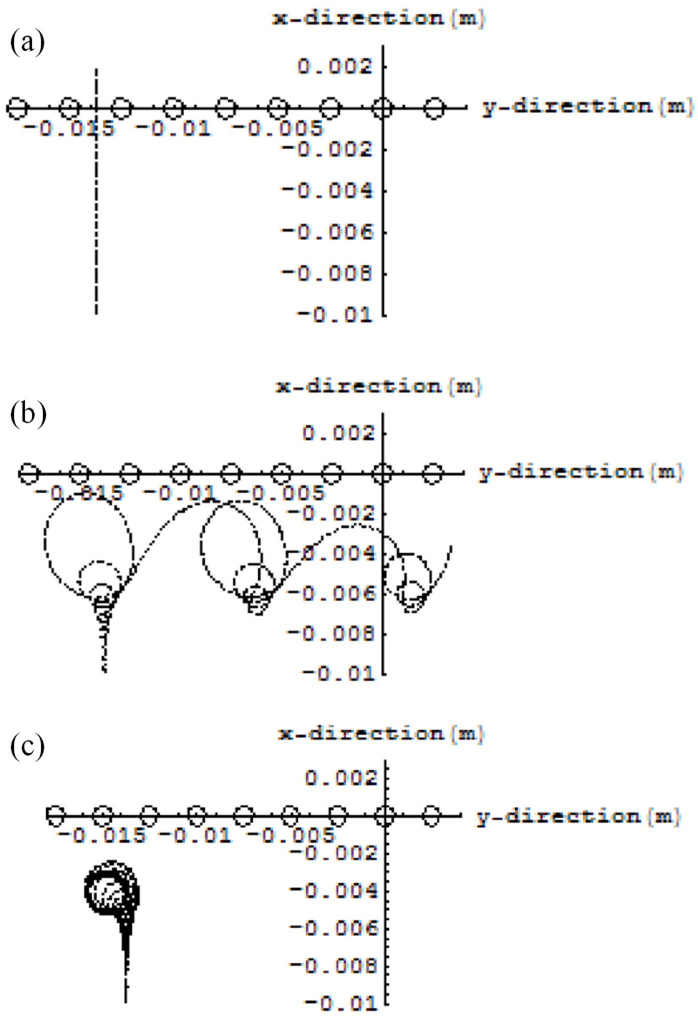

Fig. 8. Computer simulation of bubble motion: (a) slip-through, (b) traveling, and (c) stagnation modes.

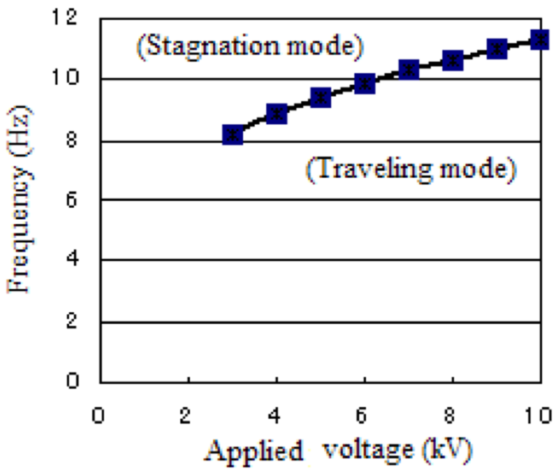

Fig. 9. Characteristics of bubble motion.

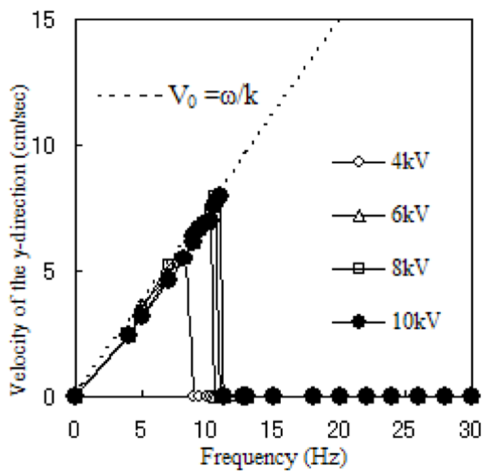

Fig. 10. Bubble drift velocity by computer simulation.

determined by computer simulation. This figure corresponds to Fig. 6 of the experimental results and presents the quantitative findings. Fig. 10 shows the velocity of the bubble in the *y*-direction (transverse direction) versus the frequency. The dotted line indicates the propagation velocity of the traveling-wave electric field, $V_0 = \omega/k$, corresponding to the experimental results in Fig. 7. Therefore, the bubble motion velocity based on the numerical solution is in good agreement with the experimental results in terms of the overall trend, although there are differences in the boundary values at which the mode transition occurs. Despite the application of a low-frequency AC electric field, no deformation is observed among the bubbles of approximately 0.2 mm diameter. Therefore, the effects of deformation are not considered in the computer simulations. However, bubble deformation is important for bubbles larger than 2–3 mm in diameter [18].

5. Conclusion

The motion of tiny bubbles injected into an insulating liquid by electrohydrodynamic action was visualized experimentally. A theoretical model explaining the behavior of the bubbles was constructed, and simulations were performed using this model. The results were summarized as follows:

(1) The motion of bubbles as small as 0.2 mm injected into kerosene can be controlled using an electric field curtain driven by a low-frequency three-phase AC high voltage. Bubble motion can be classified into three modes: slip-through, stagnation, and transport.

(2) In the transport mode, bubbles do not move continuously and smoothly. Instead, they exhibit discontinuous movement as a group of bubbles three times as wide as the electrode pitch.

(3) The electrohydrodynamic action of a bubble can be expressed by the equation of its motion in an insulating liquid, considering the Coulomb, gradient, and buoyancy forces.

The technology of controlling fine bubble motion in insulating liquids could be applied to new chemical fields, such as gas–liquid mixed phases, microgravity environments, and space applications, especially for bubble separation and bubble dwell time control.

Acknowledgements

We would like to express our deepest gratitude to the late Professors Emeriti Michio Aoyama and Motoyuki Kawasaki of the Nishinippon Institute of Technology for their cooperation in this research. The authors would like to thank Enago (www.enago.jp) for the English language review.

References

[1] Kawamoto H., and Shibata T., Electrostatic cleaning system for removal of sand from solar panels, *J. Electrostat.*, Vol. 73, pp. 65–70, 2015.

[2] Champion K., and Schaub H., Electrostatic potential shielding in representative cislunar regions, *IEEE Trans. Plasma Sci.*, Vol. 51, pp. 2482–2500, 2023.

[3] Obreschkow D., Kobel P., Dorsaz N., Bosset A. de., Nicollier C., and Farhat M., Cavitation bubble dynamics inside liquid drops in microgravity, *Phys. Rev. Lett.*, Vol. 97, 0945502, 2006.

[4] Aoyama M., Oda T., Ogihara M., Ikegami Y., and Masuda S., Electrodynamical control of bubbles in dielectric liquid using non-uniform travelling field, *J. Electrostat*, Vol. 30, pp. 247–258, 1993.

[5] Masuda S., Fujibayashi K., and Ishida K., Elektrodynamisches Verhalten aufgeladener Aerosolteilchen im inhomogenen Wechselfeld und seine Anwendungsmöglichkeiten in der Staubtechnik, *Staub-Reinhaltung der Luft*, Vol. 30, pp. 449–456, 1970.

[6] Melcher J.R., Electric field and forces in semi-insulating liquids, *J. Electrostat.*, Vol. 2, pp. 121–132, 1976.

[7] Liu G., Marshall J.S., Particle transport by standing waves on an electric curtain, *J. Electrostat.*, Vol. 68 (4), pp. 289–298, 2010.

[8] The Inst. Electrostatic Japan Ed., *Electrostatic Handbook*, pp.306-308, Ohm Co., 1981. (in Japanese).

[9] Masuda S., and Kamimura T., Approximate methods for calculating a non-uniform travelling field, *J. Electrostat*., Vol. 1 (4), pp. 351–370, 1975.
[10] Kodama H., *Charcoal Washing Theory*, p.16, Kyoritsu-Pub. Co., 1942. (in Japanese)
[11] Lamb H., *Hydrodynamics*., Dover Publications, p.571, 1945.
[12] Jones T. B., Electrohydrodynamically Enhanced Heat Transfer in Liquids - A Review, *Advances in Heat Transfer*, Vol.14, pp. 107–148, 1979.
[13] Wu. J., Understanding the electric double-layer structure, capacitance, and charging dynamics, *Chem. Rev.*, Vol. 122, pp. 10821–10859, 2022.
[14] Millikan R. A., The Isolation of an ion, a precision measurement of its charge, and the correction of Stokes's law, *Phys. Rev. (Series I)*, Vol. 32, pp. 349–397, 1911.
[15] Cross J. A. ed, *Electrostatics - Principles, Problems and Applications-*, p.81, Adam Hilger, Bristol, England, 1987.
[16] Stratton J. A., *Electromagnetic Theory*, McGraw-Hill Book Company, p.116–117, 1941.
[17] Ohta K., *Les fondements de l'électrodynamique* I, University of Tokyo Press, p.99, 2012. (in Japanese)
[18] Siedel S., Cioulachtjian S., Robinson A. J., and Bonjour J., Bubble Distortion due to EHD Stress, *Int. J. Plasma Environ. Sci. Technol*., Vol. 7, pp. 37–43, 2013.